Resonant electron - CF collision processes

C. S. Trevisan,[1] A. E. Orel,[1] and T. N. Rescigno[2]

[1]*Department of Applied Science, University of California, Davis, CA 95616*
[2]*Chemical Sciences, Lawrence Berkeley National Laboratory, Berkeley, CA 94720*

(Dated: September 8, 2005)

Electronic structure methods are combined with variational fixed-nuclei electron scattering calculations and nuclear dynamics studies to characterize resonant vibrational excitation and electron attachment processes in collisions between low-energy electrons and CF radicals. Several low-lying negative ion states are found which give rise to strong vibrational excitation and which are expected to dominate the low-energy electron scattering cross sections. We have also studied several processes which could lead to production of negative ions (F^- and C^-), however, in contrast to other recent predictions, we do not find CF in its ground state to be a significant source of negative ion production when interacting with thermal electrons.

PACS numbers: 34.80.Gs

I. INTRODUCTION

The fact that the perfluorinated gases widely used in the plasma processing of semiconductors can cause significant environmental damage has prompted a search for new plasma reactant gases whose atmospheric interactions are more benign. C_2F_4 is a gas that has low global warming potential [1]. Under electron bombardment, it fragments to produce reactive CF, CF_2 and CF_3 radicals that can etch silicon surfaces [2]. Since electron collision cross sections for these transient, reactive species are difficult to measure experimentally, *ab initio* theory can be of value in estimating the cross sections which are needed in large-scale simulations of these processing plasmas.

The spectroscopy of the CF radical has been studied by a variety of techniques over the past 50 years [3–6] and its principle emission bands have been identified and characterized [7–10]. The equilibrium geometry (R=2.44a_o) and ground state dipole moment (0.645D) have been deduced from spectroscopic analysis [5, 6, 11] and have been confirmed by several theoretical studies [12, 13]. In contrast to its electronic properties, which have been studied both theoretically [14] and experimentally [15], little is known of CF interactions with low-energy electrons. There are no experimental data on cross sections and, on the theoretical side, there is the single, recent theoretical study of e-CF collisions using the *R*-matrix method, by Rozum, Mason and Tennyson [16].

CF is an open-shell molecule with a $^2\Pi$ ground state. It is isoelectronic with NO, which has been the focus of several recent theoretical [17, 18] and experimental [19–22] studies, and might be expected to display similar behavior in its interaction with low-energy electrons. In particular, the addition of an electron to CF results in three anion states of $^3\Sigma^-$, $^1\Delta$ and $^1\Sigma^+$ symmetry, which by analogy with NO^- (and O_2) are expected to be separated by only a few eV. Rozum *et al.* [16] found that the lowest ($^3\Sigma^-$) anion state crosses the ground state CF potential energy curve close to its minimum, as is the case with NO/NO^-. Rozum *et al.* have estimated the ground state dissociative electron attachment (DEA) cross section to be about 600 ${a_0}^2$. An attachment cross section of this size - which is more than six orders of magnitude larger than the result we found for the ground state DEA cross section for NO - would have important implications for CF produced in plasma reactors. Rozum *et al.* also reported weakly bound CF^- states of $^1\Pi$ and $^3\Pi$ symmetry, for which there are no NO^- or O_2 analogs.

Despite the expected similarities between the CF/CF^- and NO/NO^- states near equilibrium geometry, there are important differences between the two systems. The electron affinity of fluorine is more than twice that of oxygen, so the threshold for DEA through the $^3\Sigma^-$ state which correlates with $C+F^-$ ($N+O^-$) in the case of CF (NO) should be correspondingly lower for CF than it is for NO. There are other key differences. The $^1\Delta$ and $^1\Sigma^+$ negative ion states, in the case of NO, correlate with $N^-(^3P)+O(^3P)$. But the electron affinity of nitrogen is essentially zero, so these states cannot serve as channels for DEA. In the CF case, the $^1\Delta$ and $^1\Sigma^+$ negative ion states dissociate to $C\ (^1D)+F^-(^1S)$, lending, in principle, two more channels for negative ion production. Finally, we note that, unlike nitrogen, carbon has a positive electron affinity of ∼1.26 eV [23], which leads one to ask whether there are negative ion resonance states that might serve as channels for C^- production.

Our purpose here is carry out an investigation of resonant low-energy electron-CF collision processes, to clarify the various states and mechanisms involved in the production of negative ions and vibrationally excited species and to quantify the magnitude of the collision cross sections. The techniques we have used include electronic structure calculations employing multi-configuration self-consistent field (MCSCF), complete active space (CAS) and multi-reference configuration-interaction (MRCI) techniques, fixed-nuclei complex Kohn variational calculations and nonlocal complex potential model calculations for the nuclear dynamics. As we shall see, while some of our findings are consistent with those of Rozum *et al.* [16], there are areas where our findings and theirs are in substantial disagreement.

The theoretical techniques we have used are briefly de-

scribed in the following section. Section III presents the computational details of the present theoretical study together with our results. We conclude with a brief discussion.

II. THEORETICAL TECHNIQUES

The parameters needed to set up a nuclear wave equation and construct resonant vibrational excitation and DEA cross sections can be obtained from an analysis of fixed-nuclei electron scattering T-matrix elements. These T-matrix elements were computed using the complex Kohn variational method [24]. In this method, the electronic trial wave function of the scattering system is expanded as

$$\Psi = \sum_{\Gamma} \mathcal{A}[\Phi_{\Gamma}(\mathbf{x}_1..\mathbf{x}_N)F_{\Gamma}(\mathbf{x}_{N+1})] + \sum_{\mu} d_{\mu}\Theta_{\mu}(\mathbf{x}_1..\mathbf{x}_{N+1}) \quad (1)$$

where the Φ_{Γ} are N-electron target eigenstates, $\mathbf{x}_i$ denote space-spin coordinates, $\mathcal{A}$ antisymmetrizes the coordinates of the target and scattered electrons and the Θ_{μ} are square-integrable $(N+1)$-electron configuration state functions (CSFs). The first sum, which we denote as the P-space portion of the wave function, includes target states that we wish to explicitly include in the close-coupling expansion. We denote the second sum as the correlation portion of the wave function. In the Kohn method, the F_{Γ}, which represent the wave functions of the scattered electron, are expanded as linear combinations of symmetry-adapted molecular orbitals and numerical continuum functions.

The $(N+1)$-electron CSFs describe short-range correlations and the effects of closed-channels and are critical to striking a proper balance between intra-target electron correlation and correlation between target and scattered electrons. Although we will focus primarily on electronically elastic processes in the present study, the P-space portion of the wave function is written as a sum to reflect the fact that the open-shell ground state of CF is a $^2\Pi$ state and thus both of its spatial components must be retained in the trial function.

Electronic structure methods can be applied for *ab initio* determination of ground- and excited-state target energies and wave functions. The same techniques can also be applied to anion states and give unambiguous values at geometries where they are electronically bound. When an anion state potential energy curve crosses above the ground state neutral curve, it becomes a complex quantity. One can nevertheless obtain a useful approximation to the real part of the resonance anion curve from such calculations, as long as the resonance is reasonably narrow and the basis set employed does not contain very diffuse functions, which invariably leads to variational collapse. The structure calculations were performed with an eye toward obtaining proper dissociation limits and reasonably accurate dissociation energies for both neutral and anion species. Where feasible, we first generated a complete active space (CAS) of orbitals from a multi-configuration self-consistent field (MCSCF) calculation. We then perform multi-reference configuration-interaction (MRCI) calculations including all single- and double-excitations from the CAS. Since it is neither numerically nor computationally feasible to employ such elaborate CI wave functions as target states in variational scattering calculations, we generally employ simpler (50-100 term) CAS wave functions for the target states in our complex Kohn calculations, using natural orbitals extracted from the more elaborate CI calculations.

Resonant nuclear dynamics was treated using the nonlocal formulation of the nuclear wave equation which we introduced in our earlier study of electron-NO scattering [18]. The nuclear wave equation at total energy E is

$$(E - K_R - V_{res})\xi_{\nu} = \phi_{\nu} \quad (2)$$

where K_R is the nuclear kinetic energy operator, V_{res} is a complex, nonlocal anion potential described below and ξ_{ν} is the nuclear wave function associated with the electronic resonance state. The driving term for the nuclear wave equation, or "entry amplitude", ϕ_{ν} is defined as

$$\phi_{\nu}(r) = \gamma^{l+1/2}(k_i, R)\left(\frac{\Gamma(R)}{2\pi}\right)^{1/2}\eta_{\nu}(R), \quad (3)$$

where η_{ν} is the initial vibrational wave function of the neutral target, $\Gamma(R)$ is the resonance width and $\gamma(k,R)$ is a barrier penetration factor, defined as

$$\gamma(k,R) = \begin{cases} k/k(R) & \text{if } k < k(R) \\ 1 & \text{otherwise} \end{cases} \quad (4)$$

where k is the physical electron momentum, and $k(R)$ is the local momentum at which the resonance would occur if electrons were scattered by molecules with the nuclei fixed at separation R,

$$k^2(R)/2 = E_{res}(R) - E_0(R), \quad (5)$$

with $E_0(R)$ denoting the electronic energy of the target. For l, we use the angular momentum quantum number that corresponds to the lowest partial wave that contributes to the resonance. The barrier penetration factor is thus introduced to insure that the computed cross sections will vanish near scattering thresholds with proper Wigner threshold behavior.

The complex anion potential that appears in our nonlocal model is defined as

$$V_{res}(R,R') = E_{res}(R)\delta(R-R') - i\pi\sum_{\nu}^{open} U_{\nu}(k_{\nu},R)U_{\nu}(k_{\nu},R'). \quad (6)$$

E_{res} is the real part of the potential energy curve of the negative ion obtained from electron-molecule scattering calculations (or bound-state calculations in its bound region), and k_ν is the momentum of the scattering electron when the molecule is left in the final vibrational state η_ν. The sum runs over the energetically open vibrational states of the ion. $U_\nu(k_\nu, R)$ is the matrix element coupling the resonance to the non-resonant background associated with a vibrational level ν and is approximated as

$$U_\nu(k_\nu, R) = \gamma^{l+1/2}(k_\nu, R) \left(\frac{\Gamma(R)}{2\pi}\right)^{1/2} \eta_\nu(R). \qquad (7)$$

At sufficiently high incident energy one can make use Eq. (4) along with the assumed completeness of the sum over vibrational states in Eq. (6) to show that the nonlocal potential in Eq. (6) limits to the local width:

$$\sum_\nu^{open} U_\nu(k_\nu, R) U_\nu(k_\nu, R') \underset{r\to\infty}{\sim} \frac{\Gamma(R)}{2\pi}\delta(R - R'). \qquad (8)$$

Thus, as the incident energy is increased above threshold, the nonlocal potential model we use here goes over to the familiar local complex potential or "boomerang" model, with the barrier penetration factor still present in the entry (and exit) amplitudes.

It should be noted that the definition of the entry amplitude given in Eq. (3) is appropriate when there is only one electronic channel into which the resonance can decay, which is typically the case with low-energy shape resonances. When the resonance can decay into more than one energetically open electronic channel, then the total width $\Gamma(R)$ in the entrance amplitude should be replaced by the partial width corresponding to the initial electronic channel [25].

Integral elastic scattering and vibrational excitation cross sections are given by

$$\sigma_{\nu\to\nu'} = \frac{4\pi^3}{k_i^2} \left|\langle\phi_{\nu'}|\xi_\nu\rangle\right|^2. \qquad (9)$$

where the "exit amplitude", $\phi_{\nu'}$, is defined as in Eq. (3), with ν' labeling the final vibrational state. Vibrational excitation and elastic cross sections calculated for each resonance state from Eq. (9) must be multiplied by their appropriate statistical weight and added. The physical cross sections for CF, as in the case of NO, are given by

$$\sigma^{total}_{\nu\to f} = \frac{1}{8}\left(3\sigma^{^3\Sigma^-}_{\nu\to f} + 2\sigma^{^1\Delta}_{\nu\to f} + \sigma^{^1\Sigma^+}_{\nu\to f}\right). \qquad (10)$$

In the case of dissociative attachment, a solution of Eq. (2) must be constructed which is regular at the origin and behaves asymptotically as a purely outgoing wave. The integrated cross section for dissociative electron attachment from vibrational state ν is then expressed as

$$\sigma_{\nu\to DA} = g\frac{2\pi^2}{k_\nu^2}\frac{K}{\mu}\lim_{R\to\infty}|\xi_\nu(R)|^2 \qquad (11)$$

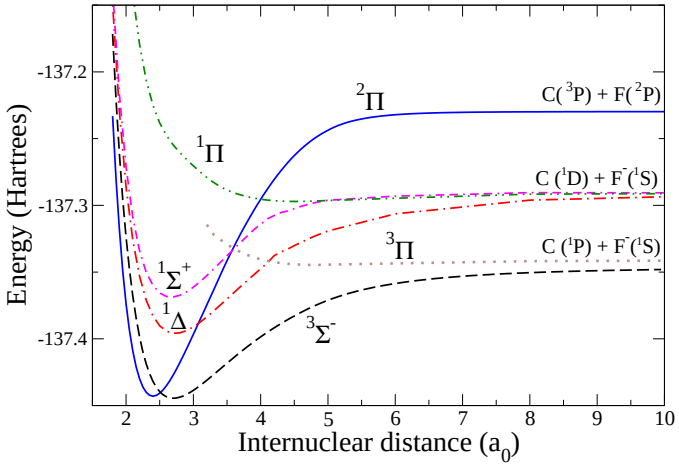

FIG. 1: (Color online) CF and CF^- potential curves. Solid curve: $^2\Pi$ neutral ground-state; dashed curve: $^3\Sigma^-$ anion; dash-dot curve: $^1\Delta$ anion; double dash-dot curve: $^1\Sigma^+$ anion; dotted curve: $^3\Pi$ state; double dot-dash curve: $^1\Pi$ state. Internuclear distances are given in atomic units, where $a_o = 5.2917721 \times 10^{-11}$ m is the Bohr radius. Energies are in units of Hartrees = 4.3597438×10^{-18} J.

where g is the ratio of resonance state to initial state statistical weights (i.e. 3/8 for the case of the $^3\Sigma^-$ resonance) and $K^2/2\mu$ is the asymptotic kinetic energy of the dissociated fragments with reduced mass μ, i.e.,

$$K^2/2\mu = E - V_{res}(R)|_{R\to\infty}. \qquad (12)$$

III. CALCULATIONS AND RESULTS

A. Neutral and anion potential curves

Structure calculations — We performed MRCI structure calculations to obtain the potential curves for both the neutral ground-state and the anion states of CF. As stated above, the same calculations were used to approximate the real parts of the resonance anion curves at geometries where they become electronically unbound. The molecular orbital basis sets for these calculations were constructed using the augmented, correlation-consistent Gaussian basis sets described by Kendall *et al.* [26].

The orbital basis for these calculations were obtained as follows. We first carried out CAS-MCSCF calculations. The active space for these calculations consisted of all the orbitals of the carbon and fluorine $1s$, $2s$ and $2p$ shells, with the electrons distributed in all possible ways. The MRCI calculations included all single- and double-excitations from the set of CAS reference configurations, with the restriction that the four core orbitals (carbon and fluorine $1s$ and $2s$) remain doubly occupied. The results of these calculations are depicted in Fig. 1.

As expected, there are similarities between these curves and those previously obtained [17, 18] for the iso-

electronic radical NO and its anion states. The ground $^2\Pi$ state of the neutral is crossed by the $^3\Sigma^-$ anion state close to its equilibrium geometry. There are two other low-lying anion states of $^1\Delta$ and $^1\Sigma^+$ symmetry which lie higher in energy and cross the neutral curve at larger internuclear separations.

Despite the similarities between CF and NO, it is worth noting several important differences. Just as in the case of NO, we expect to find a prominent resonance behavior which displays a rich structure in the elastic and vibrational excitation cross sections. Nevertheless, in the case of CF, there is a larger energy separation between the anion curves, which will leave a signature in the vibrational excitation cross sections that will be discussed in section III B.

As in the case of NO, dissociative electron attachment can produce ground state atomic fragments ($C(^3P)$ and $F^-(^1S)$ in this case) via the $^3\Sigma^-$ anion state. However, the threshold for this process is approximately 1.8 eV lower in CF, reflecting the difference between the electron affinities of F (∼3.40 eV [27]) and O (∼1.46 eV [28]). It is interesting to note that the binding energies of CF and NO are very similar, while those of the corresponding $^3\Sigma^-$ anions reflect the difference between the respective electron affinities. As we will see in section III C, the production of F^- will consequently be more efficient than in the case of O^-.

Another notable difference is that in the e^-+ CF case, there are two other channels for the production of F^-, namely through the $^1\Delta$ and the $^1\Sigma^+$ resonance states, which dissociate to $C^*(^1D) + F^-(^1S)$. The corresponding anion states in the case of NO^- correlate with $O(^3P) + N^-(^3P)$, but the electron affinity of N is negligible, so the $^1\Delta$ and the $^1\Sigma^+$ states are therefore not viable channels for DEA in the case of NO.

Figure 1 also shows curves calculated for the $^3\Pi$ and $^1\Pi$ states of CF^-, which are seen to be strictly repulsive. This contrasts markedly with the results of Rozum *et al.* [16], who found these states to be weakly dipole-bound at the equilibrium geometry of the neutral. However, at the equilibrium geometry of 2.44 a_o, the dipole moment of ground-state CF is sub-critical [11], which argues strongly against the presence of dipole-bound anion states.

In addition to the production of F^-, the collisions of electrons with CF can, in principle, also produce C^-. This will be discussed in Sec. III D.

Scattering calculations—To obtain R-dependent resonance widths for the anion states of CF, we carried out fixed-nuclei scattering calculations using the complex Kohn method. The neutral target state wave function was obtained by carrying out a CASCI calculation where the 5σ, 6σ, 1π and 2π orbitals constituted the active space. These orbitals were in turn chosen as the natural orbitals obtained from a multi-reference plus all singles calculation on the neutral ground-state. The basis set for these calculations was the Gaussian set of Kendall *et al.* [26] described above.

The $(N+1)$- electron trial function was constructed by including all CSFs generated by placing eight electrons in the four frozen core orbitals, seven electrons in the active space and one electron in the virtual space. This gave ∼5200 configurations for each symmetry considered. Scattering calculations in overall $^3\Sigma^-$, $^1\Delta$ and $^1\Sigma^+$ symmetry were carried out over a range of geometries and resonace parameters were extracted from an analysis of the eigenphase sums.

TABLE I: Resonance parameters for the three low-lying CF^- states at several internuclear separations, R. Both position (E_{res}) and width (Γ_{res}) are given in Hartrees. R is given in atomic units. The resonance positions are the energy differences between the anion and neutral states from our electronic structure calculations, while the resonance widths were obtained from fixed-nuclei scattering calculations.

CF^-	R (a_o)	E_{res}(Hartree)	Γ_{res}(Hartree)
$^3\Sigma^-$	2.150	0.0364	0.0448
	2.200	0.0314	0.0324
	2.250	0.0264	0.0233
	2.300	0.0212	0.0163
	2.350	0.0161	0.0109
	2.400	0.0111	0.0069
	2.440	0.0071	0.0044
	2.450	0.0061	0.0039
	2.500	0.0012	0.0018
$^1\Delta$	2.200	0.0767	0.1120
	2.250	0.0739	0.0836
	2.300	0.0689	0.0597
	2.350	0.0652	0.0446
	2.400	0.0600	0.0339
	2.440	0.0558	0.0274
	2.450	0.0558	0.0259
	2.500	0.0505	0.0196
	2.550	0.0460	0.0145
$^1\Sigma^+$	2.100	0.1002	0.1282
	2.150	0.0995	0.0105
	2.200	0.0958	0.0830
	2.250	0.0940	0.0670
	2.300	0.0899	0.0551
	2.350	0.0872	0.0459
	2.400	0.0829	0.0383
	2.440	0.0789	0.0329
	2.450	0.0796	0.0316
	2.500	0.0751	0.0253
	2.550	0.0713	0.0194
	2.700	0.0585	0.0059

It is not surprising that with the relatively simple target wave function employed in the Kohn trial function, the positions of the resonance states relative to the neutral target were rather sensitive to the target orbitals employed. In our earlier calculations on NO [17], we found that by using a weighted average of density matrices from calculations on both neutral and anion states in determining the target molecular orbitals, we could adjust the position of the lowest resonance state to repro-

duce the known electron affinity of NO. This strategy was not possible in the present case, since the electron affinity of CF is not known and no experimental electron-CF scattering measurements have been carrioed out. Therefore, for the nuclear dynamics calculations, only the resonance widths that were extracted from the fixed-nuclei calculations were used. For the resonance positions, we used the values of the anion energies obtained from the more extensive electronic structure calculations described above. In the case of the $^3\Sigma^-$ resonance, the scattering and structure calculations gave resonance energies near the equilibrium geometry of the neutral target that only differed by ∼0.05 eV. For the higher $^1\Delta$ resonance, the scattering calculations gave values ∼1 eV lower than the structure calculations. For the $^1\Sigma^+$ resonance, the differences were ∼1.6 eV, but this resonance, as was the case with NO, contributes negligibly to vibrational excitation. The values of the resonance parameters used in the nuclear dynamics calculations, as a function of internuclear separation, are given in Table I. We note that at r=2.44 a_o Rozum *et al.* report the position of the $^1\Delta$ resonance to be about 0.5 eV lower than what we find and a width very close to ours. For the $^1\Sigma^+$ resonance, the position they report is close to what we find, but their calculated width is approximately twice our value. Rozum *et al.* were unable to determine parameters for the $^3\Sigma^-$ resonance case at equilibrium geometry.

B. Vibrational excitation

Figure 2 shows the total and individual resonance contributions to the elastic and $\nu = 0 \rightarrow 1, 2, 3$ vibrationally inelastic cross sections obtained with the nonlocal model described in Sec. II. Individual symmetry contributions include statistical weights given in Eq. (10). Both the $^3\Sigma^-$ and $^1\Delta$ cross sections show pronounced boomerang structure, as was the case with NO. In the present case there is a larger energy separation between the two anion states and consequently the irregular structure found in NO because of overlapping resonance bands is entirely absent in the elastic and $\nu = 0 \rightarrow 1, 2$ cross sections and much less pronounced in the $\nu = 0 \rightarrow 3$ cross section. The contribution from the $^1\Sigma^+$ resonance is seen to be small and unstructured.

The $^3\Sigma^-$ peaks are narrower than the $^1\Delta$ peaks, reflecting the longer autodetachment lifetime (inverse width) of the $^3\Sigma^-$ negative ion state. Another observable consequence of the relatively longer lifetime of the $^3\Sigma^-$ resonance state is the fact that the $^3\Sigma^-$ peaks occur at the same energies in all exit channels while the $^1\Delta$ peaks shift with changing final vibrational quantum number.

C. F^- Production

As mentionaed above, there are three channels for the production of F^- that can occur by the process of dissociative electron attachment to CF. The $^3\Sigma^-$ resonance is associated with the reaction channel that produces ground state fragments of $C(^3P) + F^-(^1S)$; $^1\Delta$ and $^1\Sigma^+$ resonance states dissociate into the same excited state of C plus F^-, namely, $C(^1D) + F^-(^1S)$.

Figure 3 shows the $^3\Sigma^-$ dissociative attachment cross sections calculated using the nonlocal model described in Sec. II. The numerical solution of the working equations of this process was carried out using the finite-element DVR implementation of ECS employed in our recent investigation on electron scattering by NO (see Ref. [18] and the references therein for further details).

As mentioned above, cross sections are moderately larger here (by a factor of two, approximately) than in the analogous NO case, because the dissociation energy for the $^3\Sigma^-$ CF^- state is lower. The "shallower" potential well of the CF anion also supports fewer (autodetaching) vibrational levels than its NO counterpart, making negative ion production more efficient. The cross section for dissociative attachment to CF in its vibrational ground state is negligible, as was the case with NO, but increases rapidly as the target vibrational quantum number increases. The origin of this interesting behavior was investigated and interpreted in detail in our study of NO [18]. The dramatic enhancement is not associated with any simple classical effect. Rather, evaluation of the dissociative attachment cross section involves the overlap between a rapidly oscillating scattering function and the vibrational wave function from which the dissociation is taking place. The frequency of oscillation will be closer to the frequency of oscillation of the scattering function for higher vibrational states, producing in this way a larger overlap.

Similar enhancement in the DEA cross sections with increasing target vibrational quantum number was observed in the remaining two channels for the production of F^-. The peak values for the DEA cross sections arising from the $^1\Delta$ resonance were found to be roughly 25% of the maximum values for the $^3\Sigma^-$ channel and even smaller in the case of the $^1\Sigma^+$ resonance, but cross sections of this magnitude require highly excited target states ($> \nu = 20$). For this reason, we do do not expect the $^1\Delta$ and $^1\Sigma^+$ resonances to make a significant contribution to the production of F^- in low-temperature plasmas. Apart from an increase in the threshold energy onset for dissociation out of a particular vibrational state and an overall decrease in magnitude, the shape and behavior of the DEA cross sections for the $^1\Delta$ and $^1\Sigma^+$ resonances are similar to those illustrated in Fig. 3 for the $^3\Sigma^-$ channel and so are not shown.

D. C^- Production

Since carbon has a positive electron affinity, it is interesting to ask whether there are valence negative ion states that can be formed by electron impact that dissociate to $C^-(^4S) + F(^2P)$. This asymptote lies approximately

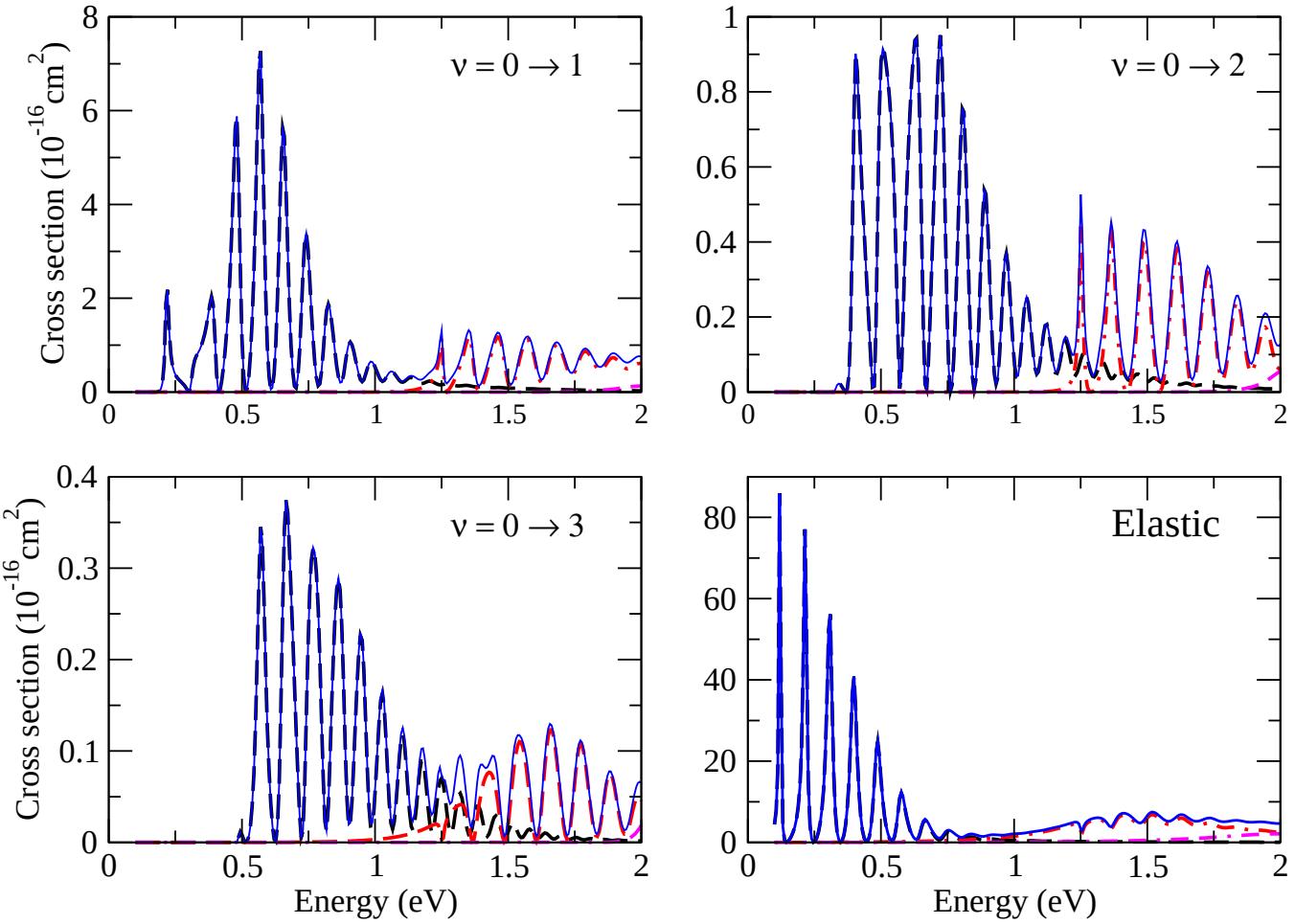

FIG. 2: (Color online) Contribution of individual resonances to the elastic and vibrationally inelastic cross sections. Solid curves: total cross sections; dashed curves: $^3\Sigma^-$ symmetry contributions; dash-dot curves: $^1\Delta$ symmetry contributions; double dash-dot curves: $^1\Sigma^+$ symmetry contributions. Individual symmetry contributions include statistical weights given in Eq. (10). Cross sections are in units of 10^{-16} cm^2. Energies are in units of eV = 1.6021765×10^{-19} J.

1.27 eV below the neutral C + F limit.

The lowest $^2\Sigma^-$ neutral state, which dissociates to ground-state C + F atoms, is nominally described by the configuration $1\sigma^2 2\sigma^2 3\sigma^2 4\sigma^2 1\pi^4[2\pi_x 2\pi_y(^3\Sigma^-)]5\sigma,^2\,\Sigma^-$ and is purely repulsive [14]. This state could in principle serve as the parent for a core-excited shape resonance with the configuration $1\sigma^2 2\sigma^2 3\sigma^2 4\sigma^2 1\pi^4[2\pi_x 2\pi_y 6\sigma(^4\Sigma^-)]5\sigma,^3\,\Sigma^-$. Note that at large internuclear distances the $2\pi_x, 2\pi_y$ and 6σ molecular orbitals correlate with the carbon 2p orbitals, while the $1\pi_x, 1\pi_y$ and 5σ molecular orbitals become the fluorine 2p orbitals. The $[2\pi_x 2\pi_y 6\sigma(^4\Sigma^-)]$ molecular orbital coupling in the anion is thus essential, since it correlates directly with the carbon anion which has the configuration $2p_x 2p_y 2p_z$,^{4}S.

There is also a $^4\Sigma^-$ neutral state, with the same orbital occupancy as the $^2\Sigma^-$ state, which dissociates to neutral C + F, but we can use the same logic employed above to discount it as a parent for resonances that correlate with C$^-$ + F. Such resonances would have the configuration $1\sigma^2 2\sigma^2 3\sigma^2 4\sigma^2 1\pi^4[2\pi_x 2\pi_y 6\sigma(^2\Sigma^-)]5\sigma,^{3,5}\,\Sigma^-$. We need not consider the $^5\Sigma^-$ anion state, since it cannot be formed by electron impact from the doublet ground state of CF. The second $^3\Sigma^-$ state, on the other hand, correlates with C$^-$ in an excited state, which is not bound. We are left with the $(...)[2\pi_x 2\pi_y 6\sigma(^4\Sigma^-)]5\sigma,^3\,\Sigma^-$ state as the only candidate for a resonance that leads to C$^-$ production. Figure 4 shows the potential curves of the $^3\Sigma^-$ core-excited anion state and its neutral parent state of symmetry $^2\Sigma^-$, together with the neutral electronic ground state of CF.

To establish whether the aforementioned anion state would appear as a shape resonance in electron+CF scattering, a simplified set of calculations was performed. We first carried out a one-channel calculation, using a single-configuration $^2\Sigma^-$ neutral target state, in overall $^3\Sigma^-$ symmetry. The use of a single-configuration target function simplifies the analysis by assuring that no

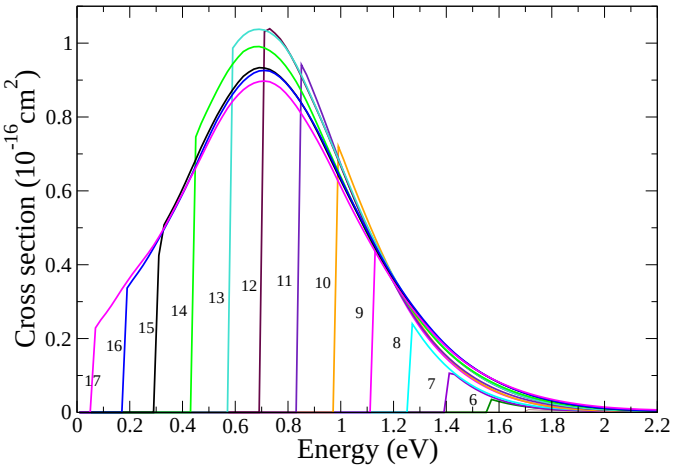

FIG. 3: (Color online) Dissociative electron attachment cross sections from vibrationally excited states 6 through 17. Cross sections are in units of 10^{-16} cm^2 and energies are in eV.

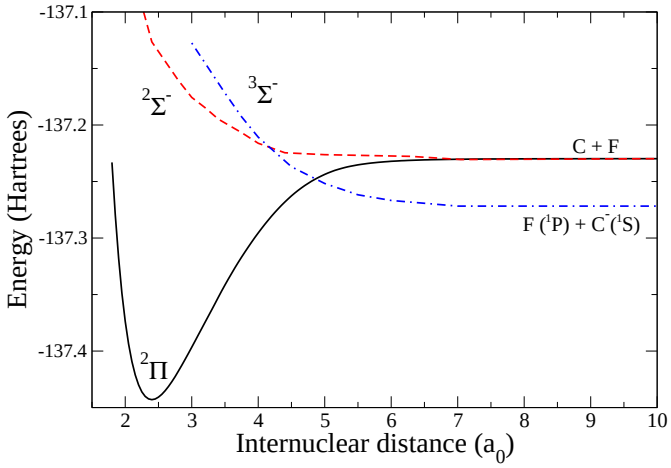

FIG. 4: (Color online) CF, CF* and CF$^-$ potential curves. Solid curve: $^2\Pi$ neutral ground-state; dashed curve: $^2\Sigma^-$ electronically excited state of neutral CF; dash-dot curve: $^3\Sigma^-$ anion state of CF. Internuclear distances are given in atomic units. Energies are in Hartrees.

unphysical pseudoresonances will appear as the result of neglecting other open electronic channels. The target orbitals for these calculations were obtained by first carrying out MCSCF calculations on the ground state of CF, followed by CAS-CI calculations for the $^2\Sigma^-$ excited state in the space of 1π, 5σ, 2π and 6σ orbitals. The natural orbitals from the latter calculation were used to form the target wave function. For the scattering calculations, we employed a "relaxed-SCF" model which includes, in addition to the static-exchange portion of the trial function, (N+1)-electron configurations obtained from spin-conserving, single-excitations of the target orbitals into virtual orbitals of the same symmetry. Such a trial function incorporates the essential short-range target distortion that accompanies resonance formation. These single-channel calculations do show a shape resonance, readily evident in the behavior of both the integral cross section and the eigenphase sum, which first appears near threshold at an internuclear separation of ∼4.0 a_0. As R is decreased, the resonance rises in energy and rapidly broadens, as seen in Fig. 5. At R=3.0 a_0, it is a very broad resonance with a position of ∼3.5 eV relative to its parent.

A second set of coupled two-state (3-channel) calculations was performed in which the ground-state $^2\Pi$ and $^2\Sigma^-$ excited target states were included in the Kohn trial function. We again used single-configuration approximations for the target states to avoid the introduction of pseudo-resonances. These calculations again indicated the presence of a core-excited shape resonance whose R-dependent width and position with respect to the $^2\Sigma^-$ target state was very close to the results obtained from the single-channel calculations. The T-matrices obtained from these calculations could be fit using a multi-channel resonance analysis to obtain the R-dependent partial widths and hence entrance amplitudes needed to estimate the dissociative attachment cross sections for producing C$^-$. However, we did not feel that such a quantitative estimate of the DEA cross sections was warranted, for the following reason.

The fact that the core-excited $^3\Sigma^-$ resonance broadens so rapidly with decreasing internuclear distance, becoming virtually undetectable at the equilibrium separation of the neutral target, might seem to imply that its capture probability would be negligibly small stating from vibrationally cold CF. On the other hand, the small-R behavior of the resonance may reflect the deficiencies of the single-configuration $^2\Sigma^-$ target state employed. Our MCSCF and CAS-CI calculations showed that the dipole moment of the $^2\Sigma^-$ target state is rather small, rising from zero at infinite separation to ∼0.2 a.u. at R=2.44. The single-configuration description of the $^2\Sigma^-$ target state, on the other hand, while dissociating properly to neutral C + F, gives a dipole moment that rises rapidly as R decreases from 4.0 a_0 to a value over 1. a.u. at R=2.44. This anomalously large dipole moment may well be responsible for the rapid broadening of the resonance at smaller R-values. A quantitatively meaningful estimate of the DEA cross section, therefore, cannot be obtained without a far more elaborate set of fixed-nuclei scattering calculations. Hence, we have identified a viable channel for producing C$^-$ ions, at electron impact energies of ∼10 eV, but are not in a position to provide a quantitatively reliable estimate of the DEA cross section.

IV. DISCUSSION

We have presented the results of a theoretical study of resonance excitation mechanisms in low-energy electron-CF collisions. In analogy with our earlier studies of

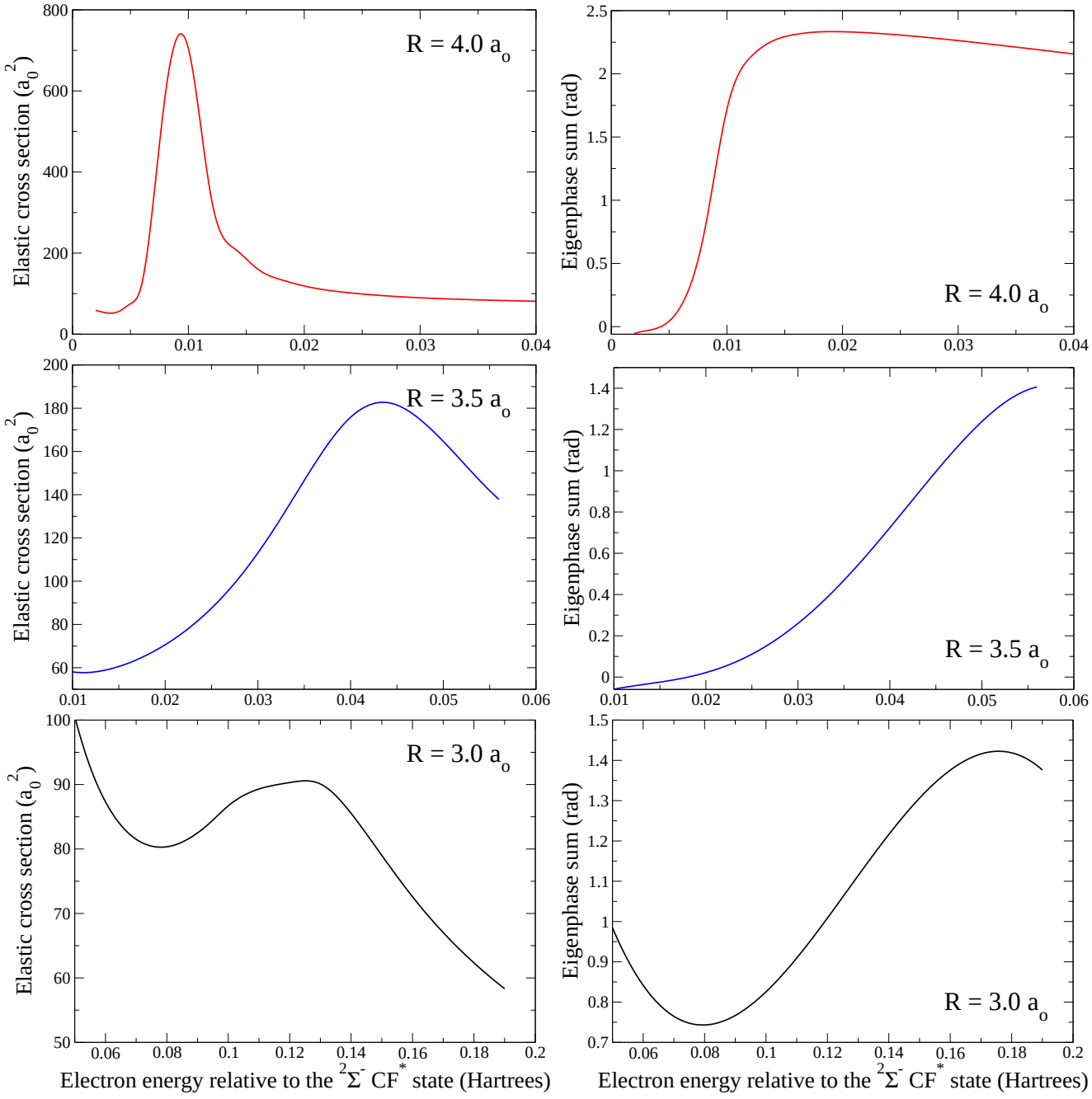

FIG. 5: (Color online) Fixed-nuclei elastic cross sections and eigenphase sums. Left panels from top to bottom: elastic cross sections at 4.0 a_0, 3.5 a_0, and 3.0 a_0. Right panels from top to bottom: eigenphase sums at 4.0 a_0, 3.5 a_0, and 3.0 a_0. Energies are given relative to the electronically excited state of CF of symmetry $^2\Sigma^-$ in Hartrees. Cross sections are in atomic units ($a_o^2 = 2.8002852 \times 10^{-21}$ m^2)

electron-NO scattering, we find three low-lying anion states of $^3\Sigma^-$, $^1\Delta$ and $^1\Sigma^+$ symmetry, the lowest two of which give rise to highly structured vibrational excitation cross sections that dominate the scattering below 2 eV. The $^3\Sigma^-$ anion curve was found to cross the ground-state neutral curve near 2.5 a_0 and dissociate to C(^{3}P) + F$^-$. The two higher anion states, which in the case of NO$^-$ do not correlate with stable negative ions, cross the neutral CF curve at larger internuclear distances and dissociate to C(^{1}D) + F$^-$. We find the $^3\Pi$ and $^1\Pi$ anion states which correlate with the C(^{3}P) + F$^-$ and C(^{1}D) + F$^-$ limits, respectively, to be strictly repulsive, in contrast to Rozum *et al.* [16] who found these states to be bound at small internuclear distances.

Dissociative attachment through the $^3\Sigma^-$ state to produce F^-, while negligible from ground-state CF, becomes significant for vibrationally excited targets above ν =6. DEA through the $^1\Delta$ and $^1\Sigma^+$ states can produce F^- and excited carbon atoms, but requires vibrationally excited targets above ν =20 to produce large cross sections. The estimate by Rozum *et al.* of a ground-state DEA cross section of $\sim$600 a_0^2 was probably based solely on the crossing of the neutral and anion curves, but failed to account for the fact that the process in energetically closed for thermal electrons.

Finally, we have identified a repulsive negative ion state which is a core-excited shape resonance associated with the $^2\Sigma^-$ excited target state. This state could lead to the production of C^- ions, but requires electrons of $\sim$10 eV. In summary, we do not expect CF to be a significant source of negative ions in low temperature plasmas.

Acknowledgments

Work at the University of California Lawrence Berkeley National Laboratory was performed under the auspices of the US Department of Energy under contract DE-AC02-05CH11231 and was supported by the U.S. DOE Office of Basic Energy Sciences, Division of Chemical Sciences. A.E.O. also acknowledges support from the National Science Foundation (Grant No. PHY-02-44911).

[1] S. Samukawa, T. Mukai, and Noguchi, Mater. Sci. Semicond. Process. **2**, 203 (1999).
[2] N. M. et al., Int. J. Mass Spectrom. **223**, 647 (2003).
[3] E. B. Andrews and R. F. Barrow, Proc. Phys. Soc. London, Sec. A **64**, 481 (1951).
[4] B. A. Thrush and J. J. Zwolenik, Trans. Faraday Soc. **59**, 582 (1963).
[5] T. L. Porter, D. E. Mann, and N. Acquista, J. Mol. Spectrosc. **16**, 228 (1965).
[6] P. K. Carroll and T. P. Grennan, J. Phys. B **3**, 865 (1970).
[7] J. P. Booth and G. Hancock, Chem. Phys. Lett. **150**, 457 (1988).
[8] J. P. Booth, G. Hancock, M. J. Toogood, and K. G. McKendrick, J. Phys. Chem. **100**, 47 (1996).
[9] T. H. Dunning, W. P. White, R. M. Pitzer, and C. W. Mathews, J. Mol. Spectrosc. **75**, 297 (1979).
[10] W. P. White, R. M. Pitzer, C. W. Mathews, and T. H. Dunning, J. Mol. Spectrosc. **75**, 318 (1979).
[11] S. Saito, Y. Endo, M. Takami, and E. Hirota, J. Chem. Phys. **78**, 116 (1983).
[12] B. A. Hess and R. J. Buenker, Chem. Phys. **101**, 211 (1986).
[13] A. P. Rendell, C. W. Bauschlicher, and S. R. Langhoff, Chem. Phys. Lett. **163**, 354 (1989).
[14] I. D. Petsalakis, J. Chem. Phys. **110**, 10730 (1999).
[15] A. Carrington and B. J. Howard, Mol. Phys. **18**, 225 (1970).
[16] I. Rozum, N. J. Mason, and J. Tennyson, J. Phys. B **36**, 2419 (2003).
[17] Z. Zhang, W. Vanroose, C. W. McCurdy, A. E. Orel, and T. N. Rescigno, Phys. Rev. A **69**, 062711 (2004).
[18] C. S. Trevisan, K. Houfek, Z. Zhang, A. E. Orel, C. W. CcCurdy, and T. N. Rescigno, Phys. Rev. A **71**, 052714 (2005).
[19] L. Josic, T. Wroblewski, Z. L. Petrovic, J. Mechlinska-Drewko, and G. P. Karwasz, Chem. Phys. Lett. **350**, 318 (2001).
[20] M. Jelisavcic, R. Panajotovic, and S. J. Buckman, Phys. Rev. Lett. **90**, 203201 (2003).
[21] M. Allan, Phys. Rev. Lett. **93**, 063201 (2004).
[22] M. Allan, J. Phys. B. **38**, 603 (2005).
[23] H. Hotop and W. C. Lineberger, J. Phys. Chem. Ref. Data **14**, 731 (1985).
[24] T. N. Rescigno, B. H. Lengsfield, and C. W. McCurdy, *Modern Electronic Structure Theory*, vol. 1 (ed. D. R. Yarkony, World Scientific, Singapore, 1995).
[25] A. E. Orel, K. C. Kulander, and T. N. Rescigno, Phys. Rev. Lett. **74**, 4807 (1995).
[26] R. Kendall, T. D. Jr., and R. Harrison, J. Chem. Phys. **96**, 6796 (1992).
[27] C. Blondel, P. Cacciani, C. Delsart, and R. Trainham, Phys. Rev. A **40**, 3698 (1989).
[28] D. M. Neumark, K. R. Lykke, T. Anderson, and W. C. Lineberger, Phys. Rev. A **32**, 1890 (1985).